EPJ Web of Conferences **268**, 00007 (2022) https://doi.org/10.1051/epjconf/202226800007
LNES 2021

Electrocatalysis with quantum chemistry

Kalishankar Bhattacharyya(*)

Department of Molecular Theory and Spectroscopy, Max-Planck-Institut für Kohlenforschung, Kaiser-Wilhelm-Platz 1, 45470 Mülheim an der Ruhr, Germany

Summary. — The following article presents a brief introduction to modeling an electrochemical reaction. Two crucial concepts, oxidation-reduction and acid-base reactions, are briefly illustrated to understand the structural changes of the electrocatalyst. These two concepts are applied to compute the stability of catalysts for electrochemical reactions from the density functional theory calculations.

1. – Introduction

Electrocatalysis is one of the forefront leading technologies to store intermittent energy and its transformation to valuable chemicals [1]. Significant interest from academic and industrial research efforts has been increased to utilize the full potential of electrocatalysts for maximum productivity, sustainability, and stability of the catalyst materials [2]. Electrochemical reactions, including water splitting reactions (oxygen and hydrogen evolution reaction), carbon dioxide reduction, and nitrogen reduction, are among the most important reactions for developing sustainable energy storage solutions [3-7]. Proton

(*) E-mail: ksb@kofo.mpg.de

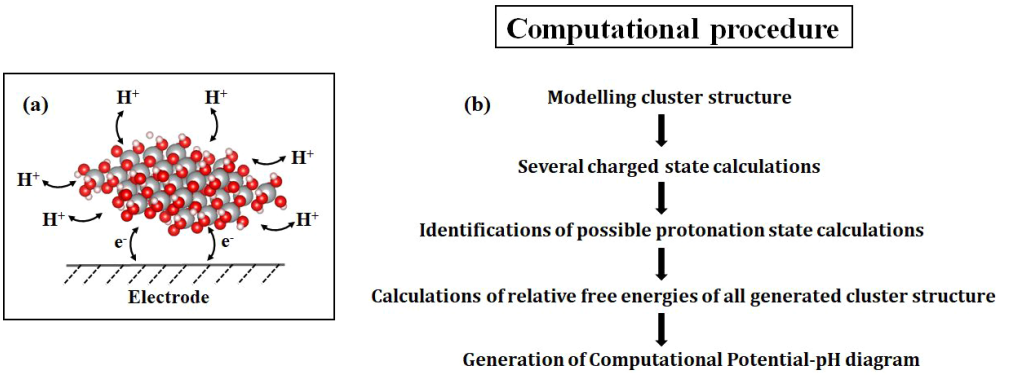

Fig. 1. – (a) Modeling of electrocatalytic materials, including the effect of potential and pH. An electrode is held for the electron transfer, and proton transfer is studied using an implicit solvation model. (b) Computational protocol for the calculations of the potential and the effect of pH of an electrocatalytic reaction.

transfer (PT), electron transfer (ET), and successive proton-coupled electron transfer (PCET) are the fundamental basis of these electrochemical reactions [8, 9]. Therefore, unique aspects of the electrocatalysts are based on controlling these proton/electron transfer kinetics and thermodynamics, which are regulated by the reaction conditions, including electrode potential, temperature, concentrations, and electrolyte [10, 11]. In this regard, computational modeling based on a predictive-quality framework in addition to experimental results has represented a pivotal role for catalysts design and optimization with atomic-scale mechanistic insights [12, 13].

2. – Computational modeling of electrocatalytic reactions for finite-size systems

As shown in fig. 1, the effect of potential and pH on the amorphous structures considering the exchange of electrons with an electrode and protonation/deprotonation with a solvent are considered simultaneously. Upon changing the potential and pH, charged states (electron transfer with the electrode) and protonation states (proton transfer with the water around the cluster) of the catalysts also change. We provide a detailed computational modeling to incorporate the effect of potential and pH in the next section.

3. – Influence of potential: determination of E^0

This section outlines our methodology to compute the effect of potential that is conceptually different from the widely applied constant charge method [14]. In the standard DFT calculations, the number of electrons is kept constant during the simulations, and the electrochemical potential can be tuned by varying the proton-coupled electron transfer (constant charge method). On the other hand the electrode potential in our approach

is a pre-set variable and can be kept constant through changing the number of electrons independently of the proton transfer (constant potential method) [15, 16].

The main reason for applying the potential to the cluster structures in exchange with an external electron reservoir (electrode) is to determine the charges state of the system that has to be the lowest energy at a specific potential. Therefore, the electrode potential can be tuned by varying the number of electrons as shown in eq. (1). On the other hand, the applied potential can thus alter the direction of equilibrium either towards A^q or A^{q-1}. Therefore, other charge states also need to be considered to find the most stable charged structures at a given potential:

$$A^q + e^- \rightleftharpoons A^{q-1}. \tag{1}$$

Computationally, we optimize all possible charged structures with an implicit solvation model and compute their energy difference. Note that the energy difference between the two charged states, A^q and A^{q-1} is equivalent to the energy requirement of the electron transfer that corresponds to the potential of an electron, *i.e.*, to the electron in *a* vacuum. It is essential to mention that reference electrodes (RHE or SHE electrode) are considered during an experimental measurement. Henceforth, reference values should be regarded throughout the potential calculations to compare the computational data with experimental results. Trasatti proposed $-4.44\,\text{eV}$ as a reference value for SHE electrodes [17]. Recently, Isse and Gennro reported $-4.28\,\text{eV}$ by measuring the solvation free energy of a proton [18]. Although the reference value so far has been reported ranging from $-4.05\,\text{eV}$ to $-4.85\,\text{eV}$ in the literature, and it is still debated which value is most reliable. Taken $-4.28\,\text{eV}$ as a reference value, the equilibrium potential *vs.* SHE can be expressed as

$$E^0{}_{V\ vs.\ SHE}(A^q/A^{q-1}) = -(\mu(A^{q-1}) - \mu(A^q)) - 4.28\ [\text{eV}]. \tag{2}$$

Equation (2) is the general expression of the electrode potential on the scale of SHE, and these values will be defined as the stable boundary region of the respective charged states as shown in fig. 2(a).

4. – Influence of *p*H: determination of pK_a

Now, we discuss how the effect of *p*H is modeled in our computational methodology to understand the impact of electrolytes. Like the electrode potential computations, the effect of *p*H of a given electrolyte on the cluster structure is to identify the protonation sites with the lowest free energy at a specific *p*H. In this way, the thermodynamic equilibrium of the acid-base reactions will be established as follows:

$$AH^{q-1}_{n-1} + H^+ \rightleftharpoons AH^q_n, \tag{3}$$

where AH^q_n is acid and its conjugated base is AH^{q-1}_{n-1}. Therefore, several protonation sites will be computed to estimate the stability region by computing the pK_a values.

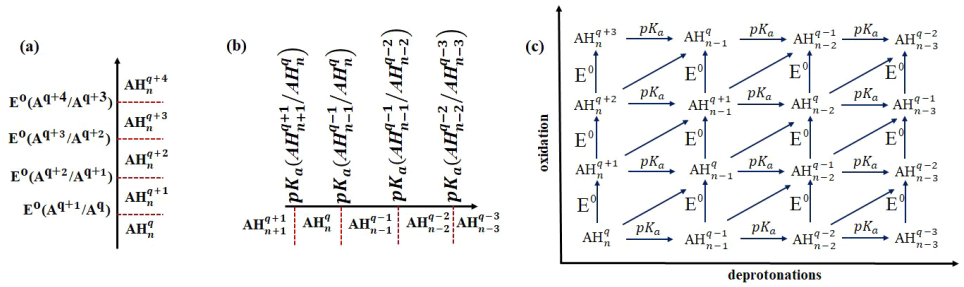

Fig. 2. – (a) Schematic description of each charge state for a potential domain with the corresponding reduction potentials. (b) Schematic depiction of each protonation state for the pH region of stability with the corresponding pK_a values as boundaries. (c) Schematic description of the two-dimensional phase diagram based on the oxidation-reduction and protonation-deprotonation reactions.

pK_a values of cluster models are calculated according to

$$pK_a = \frac{\mu(AH_{n-1}^{q-1}) + \mu_{\text{eff}}(H^+) - \mu(AH_n^q)}{RT\ln(10)}. \tag{4}$$

These values are applied to set the boundaries of the pH domain of each protonation site for the cluster, as shown in fig. 2(b).

5. – Computational potential-pH diagram: relative stability of the electrocatalyst

Based on the above methodology for the computations of potential and pK_a values for cluster structures, we now started adding and removing electrons and protons from the cluster independently and computing the potential for each electron transfer and pK_a for the proton transfer step. Hence, a two-dimensional phase diagram will be generated based on the boundaries of potential and pK_a values, as shown in fig. 2(c). This two-dimensional phase diagram will provide a stable regime based on potential and pK_a. However, to find the thermodynamic stabilities of the cluster at a particular potential and pH, we need to compute their relative stabilities with respect to the reference state: on eq. (5):

$$\begin{aligned}\Delta_r G_{AH_m^x}(AH_n^y) = {} & \mu(AH_n^y) - \mu(AH_m^x) + (m-n)\mu_{\text{eff}}(H^+) \\ & - (m-n)RT\ln(10)p\text{H} - (y-x+m-n)(U+4.28)\ [\text{eV}].\end{aligned} \tag{5}$$

Based on eq. (5), the lowest energy structures for a given potential and pH can be generated, and stable charged structures with available protonation sites of the cluster are easily identified. For a range of potential and pH, if these computations are carried out, the most stable cluster structure is specified in the three-dimensional computational

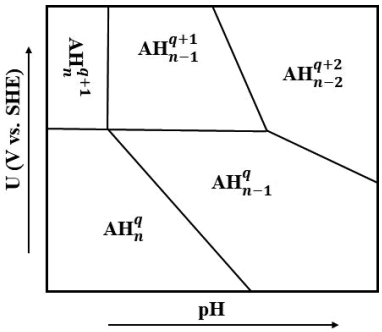

Fig. 3. – Computational potential-pH diagram describing the most stable structures based on the potential and pH scale.

potential-pH diagram as depicted in fig. 3. The interested reader can look at refs. [19] and [20] for detailed applications of the proposed methodology into the electrocatalytic reactions.

6. – Summary

This article presented a brief primer about incorporating the potential and the effect of pH on the electrocatalyst materials using electronic structure calculations. Based on the explicit consideration of the potential and the implicit consideration of the solvent effect for pH in our methodology, a computational framework is employed to investigate the structural changes of the model cluster structure. Consequently, the effect of the potential after the computations of the energetics of the neutral systems in *a posteriori* way is not required. Investigating the electron transfer through the explicit consideration of the potential and protonation-deprotonations process using the implicit solvation model will allow us to explore the electrocatalytic reactions.

* * *

The author thanks Professor Alexander A. Auer for his supervision to work on this problem and acknowledge the support from Alexander Von Humboldt Foundation for post-doctoral fellowship and Max Planck Society for computational facilities.

REFERENCES

[1] Bard A. J. and Faulkner L. R., *Electrochemical Methods: Fundamentals and Applications*, 2nd edition (John Wiley & Sons, Inc., New York) 2001.
[2] Hagen J., *Industrial Catalysis: A Practical Approach*, 2nd edition (Wiley-VCH, Weinheim, Germany) 2006.
[3] Trasatti R. S., *J. Electroanal. Chem.*, **39** (1972) 163.
[4] McCrory C. C., Jung S., Peters J. C. and Jaramillo T. F., *J. Am. Chem. Soc.*, **135** (2013) 16977.

[5] Rong X., Parolin J. and Kolpak A. M., *ACS Catal.*, **6** (2016) 1153.
[6] Montoya J. H., Tsai C., Vojvodic A. and Nørskov J. K., *ChemSusChem*, **8** (2015) 2180.
[7] Bhattacharyya K. and Datta A., *Phys. Chem. Chem. Phys.*, **21** (2019) 12346.
[8] Solis B. H. and Hammes-Schiffer S., *Inorg. Chem.*, **53** (2014) 6427.
[9] Koper M. T., *Chem. Sci.*, **4** (2013) 2710.
[10] Horvath S., Fernandez L. E., Soudackov A. V. and Hammes Schiffer S., *Proc. Natl. Acad. Sci. U. S. A.*, **109** (2012) 15663.
[11] Man I. C., Su H. Y., Calle-Vallejo F., Hansen H. A., Martinez J. I., Inoglu N. G., Kitchin J., Jaramillo T. F., Nørskov J. K. and Rossmeisl J., *ChemCatChem*, **3** (2011) 1159.
[12] Nørskov J. K., Bligaard T., Rossmeisl J. and Christensen C. H., *Nat. Chem.*, **1** (2009) 37.
[13] Seh Z. W., Kibsgaard J., Dickens C. F., Chorkendorff I., Nørskov J. K. and Jaramillo T. F., *Science*, **355** (2017) 146.
[14] Norskov J. K., Rossmeisl J., Logadottir A., Lindqvist L., Kitchin J. R., Bligaard T. and Jonsson H., *J. Phys. Chem. B*, **108** (2004) 17886.
[15] Lozovoi A., Alavi A., Kohanoff J. and Lynden-Bell R., *J. Chem. Phys.*, **115** (2001) 1661.
[16] Hörmann N. G., Andreussi O. and Marzari N., *J. Chem. Phys.*, **150** (2019) 041730.
[17] Trasatti S., *Pure Appl. Chem.*, **58** (1986) 955.
[18] Isse A. A. and Gennaro A., *J. Phys. Chem. B*, **114** (2010) 7894.
[19] Poidevin C. and Auer A. A., *Carbon*, **171** (2021) 618.
[20] Bhattacharyya K., Poidevin C. and Auer A. A., *J. Phys. Chem. C*, **125** (2021) 4379.